Proceedings of the Korean Nuclear Society Spring Meeting

Kori, Korea, May 2000

Flow-Accelerated Corrosion Behavior of SA106 Gr.C Steel in LiOH Solution using Rotating Cylinder Electrode

Jun Hwan Kim, Sang Gyu Lee, In Sup Kim

Department of Nuclear Engineering,

Korea Advanced Institute of Science and Technology,

373-1 Kusong-dong, Yusong-gu, Taejon, Korea, 305-701

Abstract

Flow-Accelerated Corrosion behavior of SA106 Gr.C steel in room temperature alkaline solution simulating CANDU primary water condition was studied using Rotating Cylinder Electrode. Systems of RCE were set up and related electrochemical parameters were applied at various rotating speeds. Corrosion current decreased up to pH 10.4 then it increased rapidly at higher pH. This is due to the increasing tendency of cathodic and anodic exchange half-cell current. Corrosion potential shifted slightly upward with rotating velocity. Passive film was formed from pH 9.8 by the mechanism of step oxidation of ferrous species into hydroxyl compound. Above pH 10.4, film formation process was active and the film became stable. Corrosion current showed some increment at the intermediate rotating speed. But it dropped at higher rotating speed because bubbles generated by circulating vortices hindered the metal-electrolyte reaction. Nevertheless, it was confirmed that RCE is an effective device to evaluate the flow induced corrosion behavior provided that the effect of flow instabilities in RCE cell can be avoided.

1. INTRODUCTION

Flow-Accelerated Corrosion (FAC) is a process where protective oxide layer on carbon or low-alloy steel dissolves into a stream of flowing water or a water-steam mixture. The oxide layer becomes thinner and less protective. Eventually a steady state is reached where the dissolution and removal rates are equal, and the stable corrosion rates are maintained. A thinned component would typically fail due to overstress from operating pressure or abrupt changes in conditions such as waterhammer, start-up loading, and so on. It was first appeared in nuclear power plant by the condensate system failure in Surry, resulted in several casualties. After the accidents, numerous components, such as feedwater system in Trojan, moisture separate drains failure at Millstone 3 Unit, suffered problem of FAC and it is now defined as a main degradation stressor on secondary piping in PWR, as well as high cycle fatigue [1,2]. Thus FAC mechanism and life management system in secondary piping have been established by the many researchers since the accident of Surry.

Whereas FAC problems in CANDU did not emerged because the condition which operates higher pH and temperature than PWR seemed to be far from the FAC compared to the feedwater corrosion in PWR until Point Lepreau feeder leak accidents happened. After AECL's recommendation for periodic monitoring feeder wall thickness, Gentilly-2, Embalse, Pickering, and Wolsong reported the same problem related to FAC [3]. And it is recognized as potential hazard in CANDU primary heat transport system because its mechanisms are not fully understood, not to mention of investigating corrosion behavior in simulated environments.

The objectives in this study are to observe FAC behavior in low alloy piping steel simulated CANDU primary coolant condition using RCE, and to study on the corrosion phenomena with the flow rate and solution pH in terms of initial passive layer formation.

2. EXPERIMENTAL PROCEDURES

2-1 Corrosion experiment

To observe fundamental electrochemical parameters in CANDU primary coolant conditions, polarization test (potentiodynamic test) was conducted. Electrochemical data were measured through the three-electrode system using EG&G model 362 scanning potentiostat. Scan rate was 0.5mV/sec. The reference electrode and auxiliary electrode were Saturated Calomel Electrode and graphite, respectively. Water chemistry condition in this study followed the CANDU primary water coolant conditions. Thus experimental solution was composed of distilled water and lithium hydroxide (LiOH). All conditions in this study were de-aerated by nitrogen gas injection for 3 hours and pH of the solution was selected as 9.84, 10.4, 10.6, 11.06, and 11.83 by the step titration of 1M LiOH. To obtain better conductivity and alleviate large IR drop across pure water, dilute PWR primary water condition was introduced to neutral solution in pH 6.96 [4]. Test material used in this study is SA106 Gr.C steel, where it shows similar chromium content and microstructure to SA106 Gr.B steel which is actually used as feeder materials. Corrosion current was measured by both Tafel extrapolation and linear polarization method around the corrosion potential.

2-2 Rotating Cylinder Electrode (RCE) experiment.

RCE is a device which contains cylindrical electrode in corrosion cell to measure the effect of flow on the corrosion behavior by the circumferentially induced flow of the rotating cylinder. Initially the device was used in chemical engineering for the purpose of electrorefining and electrodeposition study, it is now applied in FAC field because it is cost-effective, easily produces turbulent flow, generates reproducible uniform current distribution, and so on [5]. Figure 1 shows a schematic diagram of RCE setup. Spring-pushed bridge was contacted to rotating bar for the extraction of electric signal and application to external potential into working electrode. To diminish IR drop variation during the entire test period, reference electrode was inserted in an inclined position and fixed as close as possible to maintain constant distance between each electrode. All specimens were ground with emery paper, and finally polished up to the 6μm grit, de-

greased by acetone and conducted cathodic charging in –1,000mV(SCE) to remove initially given oxide on the specimen prior to the experiment. The area of working electrode was 4.71cm^2. Working electrode was taken from the orientation in which the coolant actually flowed. To avoid edge effect which is the distortion of flow near the edge of the rotating electrode, teflon cylinder was attached, whose thickness is ten times larger than working electrode. Motor used in this study was VEXTA FBL-220A model. Corrosion potential was decided to the point where anodic half-cell current (i_a) and cathodic half-cell current (i_c) are equal. Corrosion current was measured through linear polarization method.

3. RESULTS AND DISCUSSIONS

3-1 Polarization results

Figure 2 shows a potentiodynamic results with increasing pH. Metal simply dissolves in the anodic potential regime at neutral condition, showing no passive film formation on the surface. Meanwhile, it was formed in an incomplete manner from pH 9.84. Above pH 10.4, the film appeard stable from the observation of the average film current density.

Figure 3 shows the corrosion current plot with the function of pH. In this figure, corrosion current calculated both of Tafel and linear polarization. They showed more or less as a parabolic shape with the local minima at pH 10.4. This seems to be inconsistent with the conventional weight loss data of mild steel in high pH solutions [6]. Such an increasing tendency of corrosion current above pH 10.4 can be explained by the electrochemical nature of alkaline corrosion [7], which governed the kinetic reaction of iron electrode like;

Anodic half-cell reaction :

$$Fe + 2OH^- \rightarrow Fe(OH)_2 + 2e^-$$

$$i_a = 2k_a F[OH^-]\exp\{2FE/RT\}$$

Cathodic half-cell reaction : $H_2O + e^- \rightarrow \frac{1}{2}H_2 + OH^-$

$i_c = -k_c F[H_2O]\exp\{-FE/RT\}$

k_a, and k_c denote anodic and cathodic reaction rate constant. In case of increasing hydroxyl ion concentration, each anodic and cathodic half-cell current increases such that entire corrosion exchange current increases on the bare metal surface near the corrosion potential, in which both anodic and cathodic reaction may compete. When the passive film are formed, such a potential transient current will drop to a stable value, which causes suppressing metal loss.

3-2 RCE results

Figure 4 is the polarization curve with rotating velocity in neutral solution. It was observed that both the corrosion potential and the dissolution current at anodic regime augment with rotating velocity. The reason why corrosion potential shifts upward with rotating velocity may be due to the migration of reducing agent on the metal electrode more easily with the turbulent flow [8].

A bypass circuit has been installed as in figure 5(a) to investigate if contact resistance and its related thermal resistance between the bridge and rotating bar can affect the total current in given RCE system. Their equivalent circuit is modeled in figure 5(b). Result of potential value at each junction point is shown in figure 6. It can be shown that V_1 which exerts driving force of overall corrosion process and V_2 which represents open-circuit potential are almost equal during the test period. Thus it seems that effect of such resistance on the entire corrosion current is negligible compared to the solution resistance.

3-3 Effect of pH

Figure 7 shows polarization curve with increasing pH. As seen from this figure, two characterized peaks appeared at the anodic active-passive transition potential. Similar results were reported by Zhou who studied corrosion behavior of mild steel at concentrated NaOH solutions [9]. He proposed that first anodic peak combined three

parallel processes, which were composed of active dissolution of iron to a soluble bi-valent ion product of $HFeO_2^-$, formation of a surface layer and passive film, and formation of a soluble tri-valent iron species of FeO_2^- prior to the onset of passivation, and second anodic process represented the oxidation of the Fe_3O_4 magnetite film to Fe_2O_3, FeO_2^-. Proposed electrode reactions at each anodic potential based on our experimental results are as follows [9, 10] ;

First peak : E(vs. SHE) = 0.925 – 0.114pH

$$3Fe(OH)_2 + 2OH^- \rightarrow Fe_3O_4 + 4H_2O + 2e^-$$

E = – 0.114 – 0.059pH

$$Fe(OH)_2 + 2OH^- \rightarrow FeO_2^- + 2H_2O + e^-$$

E = 0.786 + 0.059log[FeO_2^-] – 0.118pH

Second peak : E(vs. SHE) = 1.387 – 0.142pH

$$Fe_3O_4 + H_2 + 2OH^- \rightarrow 3(g - FeOOH) + H^+ + 3e^-$$

E = 1.916 – 0.019logP_{H2} – 0.059pH

$$Fe_3O_4 + 4OH^- \rightarrow 3FeO_2^- + 2H_2O + e^-$$

E = 2.411 + 0.177log[FeO_2^-] – 0.236pH

3-4 Effect of flow pattern

Figure 8 is the result of linear polarization with different pH conditions and rotating velocities. Corrosion current showed larger value at 1000~2000rpm than at quiescent condition. But it dropped to the initial value at 3000rpm. Figure 9 is the flow patterns of the given RCE system. From still condition to 1000rpm, no visible change is seen around the rotating cylinder. At 2000rpm small bubbles generated and flowed concurrently near the electrode. Such bubbly flow may have an influence on entire corrosion process with a function of mixing action, causes diffusion boundary layer to be narrower. At 3000rpm, these micro-bubbles coalesced and formed annular flow, caused hindrance against corrosion reaction. Such bubbles may be resulted from the collapse of water blanket generated by Tylor vortices [11]. From those results it can be

inferred that steam quality which generated in the end part of pressure tube seems to have some effect on actual feeder corrosion by means of enhancing mass transfer, regardless the stability of the magnetite film, which greatly depends on operating water chemistry.

4. CONCLUSIONS

1. Corrosion current decreased up to pH 10.4 but it soon increased with the pH. This is due to the tendency of alkaline corrosion with the increase of each reacting concentration.

2. Corrosion potential and anodic dissolution current slightly increased with rotating velocity in neutral condition. This resulted from the diffusion enhancement of the oxidizing agent.

3. Passive film formed from pH 9.8, its nature was stable up to pH 10.4. The formation is based on the mechanisms of oxidation of ferrous species into hydroxyl compounds

4. Corrosion current showed a peak at intermediate rotation speed. But it soon dropped over high turbulence range. This seems that micro-bubbles which are generated around rotating metal surface may help corrosion action in terms of mixing action to a certain extent. On the other hand, such bubbles coalesce each other, result in hindering corrosion mechanisms at higher speed.

5. ACKNOWLEDGEMENT

The work was supported by the Brain Korea 21 project

6. REFERENCE

[1] B. Chexal, et al., *Flow-Accelerated Corrosion in Power Plant*, EPRI, TR-106611 (1996)

[2] V. Shah, and P. E. Macdonald, *Aging and Life Extension of Major Light Water Reactor Components*, 523 (1993)

[3] K. A. Burill, and E. L. Cheluget, *Corrosion of CANDU Outlet Feeder Pipes*, JAIF Int' l Conf. On Water Chemistry, 699 (1998)

[4] J. H. Kim and I. S. Kim, *Environmentally Assisted Crack Growth Behavior of SA508 Cl.3 Pressure Vessel Steel*, Proc. of the KNS Spring Meeting, 154, (1998)

[5] M. Eisenberg, et al., *Ionic Mass Transfer and Concentration Polarization at Rotating Electrode*, J. of Electrochem. Soc., **101**, 6, p.306 (1954)

[6] D. A. Jones, *Principles and prevention of CORROSION*, 357 (1992)

[7] J. Y. Zou, and D. T. Chin, *Mechanism of Steel Corrosion in Concentrated NaOH Solutions*, Electrochimca Acta, **32**, 12, 1751 (1987)

[8] Y. J. Kim, C. C. Lin, and R. Phathania, *Electrochemical Corrosion Potential Measurement with a Rotating Cylinder Electrode in 288°C Water*, Proc. Of the Water Chemistry of Nuclear Reactors System 6, 139, BNES (1992)

[9] J. Y. Zou, and D. T. Chin, *Anodic Behavior of Carbon Steel in Concentrated NaOH Solutions*, Electrochimica Acta, **33**, 4, 477 (1988)

[10] T. Misawa, *The Thermodynamic Consideration for Fe-H_2O System at 25 °C* Corr. Sci., **13**, 659 (1973)

[11] K. D. Effird, et al., *Correlation of Steel Corrosion in Pipe Flow with Jet Impingement and Rotating Cylinder Tests*, Corrosion, **49**, 12, 992 (1993)

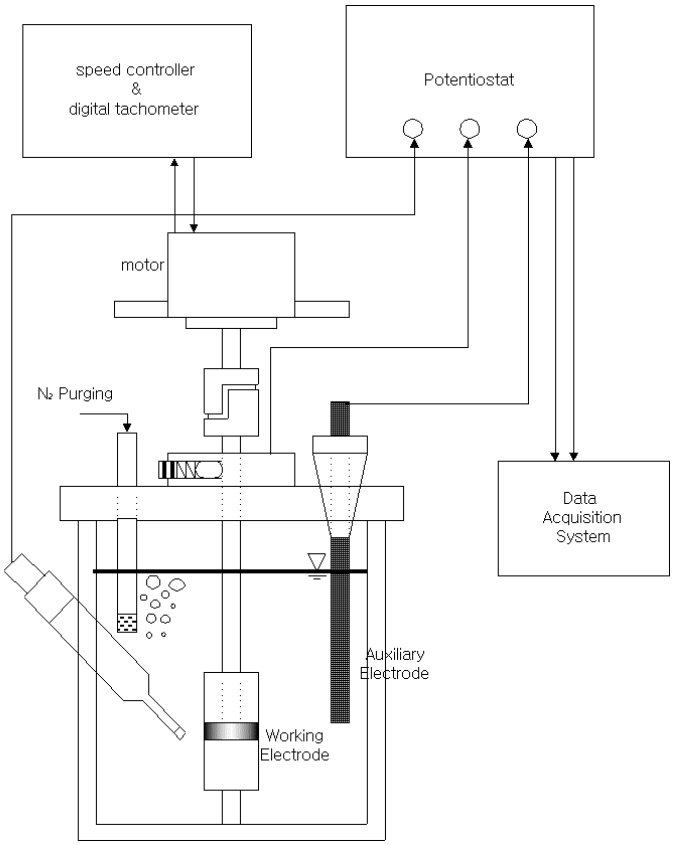

Figure 1. Schematic illustration of RCE setups

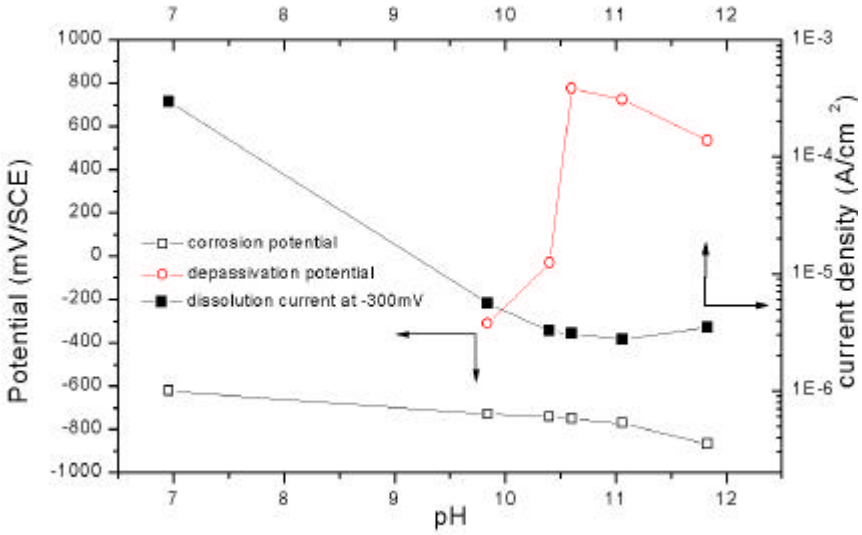

Figure 2. Electrochemical results of SA106 Gr.C steel in static condition

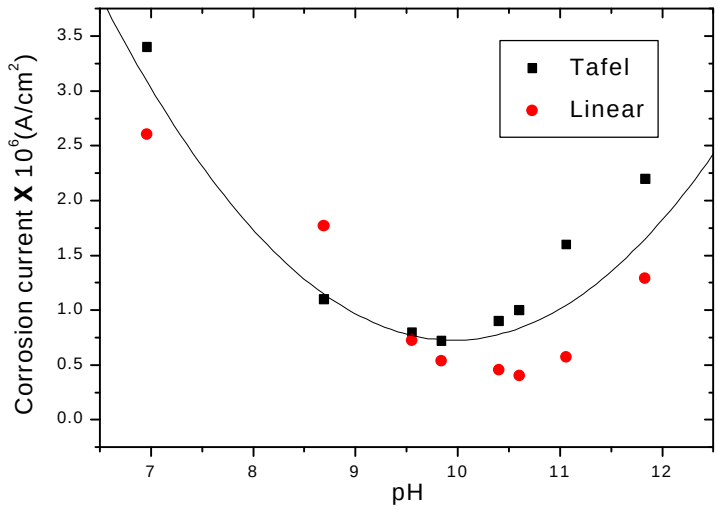

Figure 3. Result of Tafel and linear polarization with the different of pH in static condition

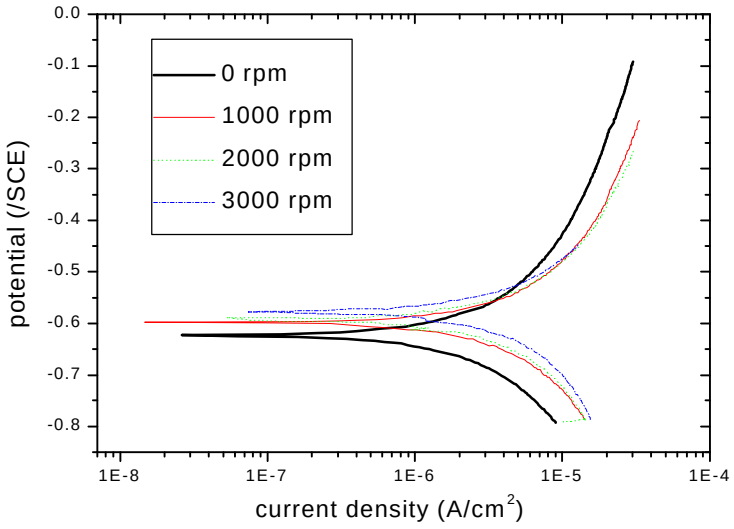

Figure 4. Results of RCE in neutral solution

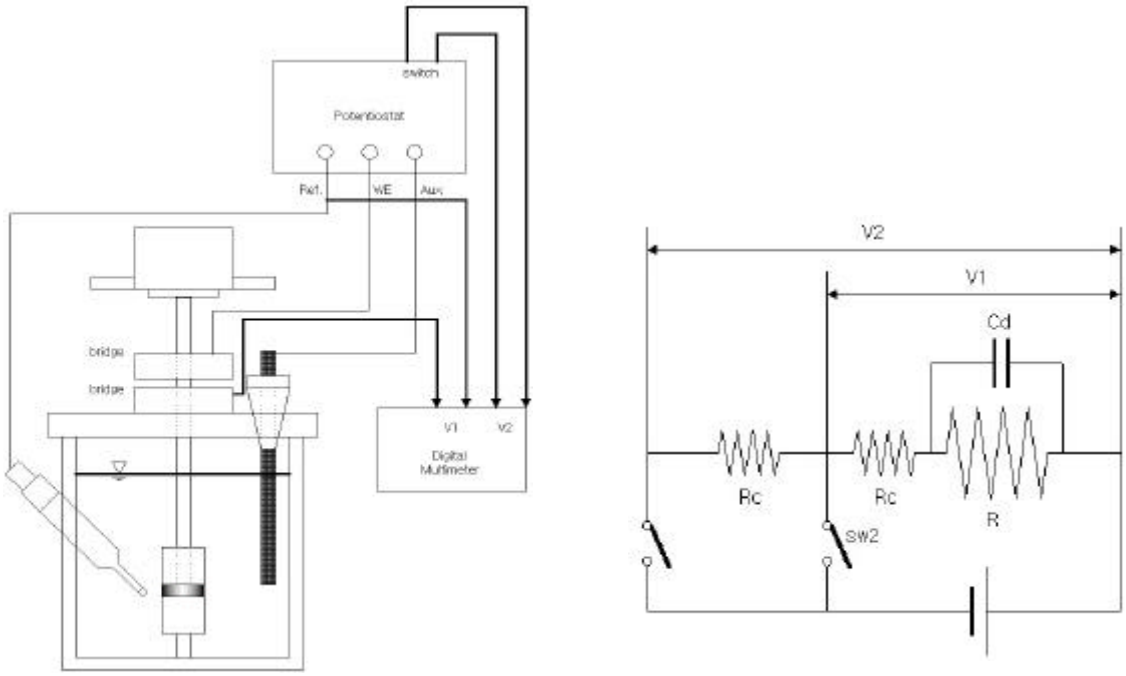

(a) (b)

Figure 5. (a) Bypass (b) Equivalent circuit for the effect of contact resistance

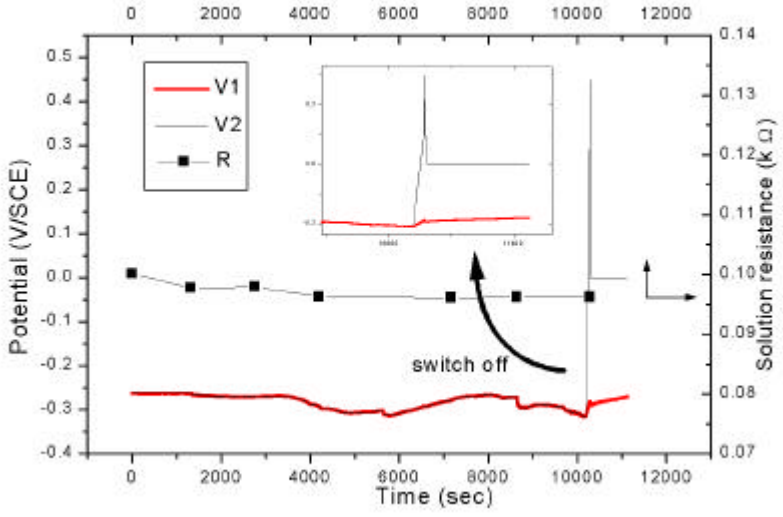

Figure 6. Effect of contact resistance in given RCE system. Solution pH was set to 12.1

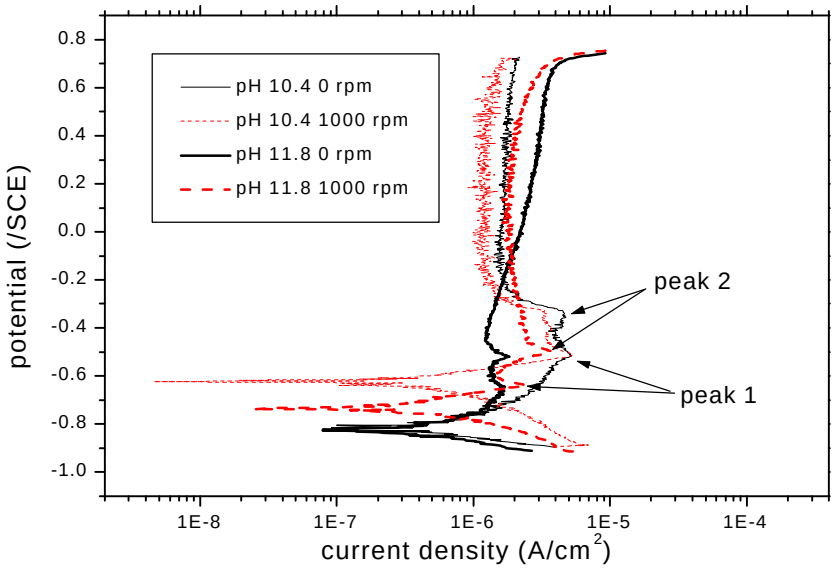

Figure 7. Polarization curves in pH 10. 4 and 11.8 at rotating velocities

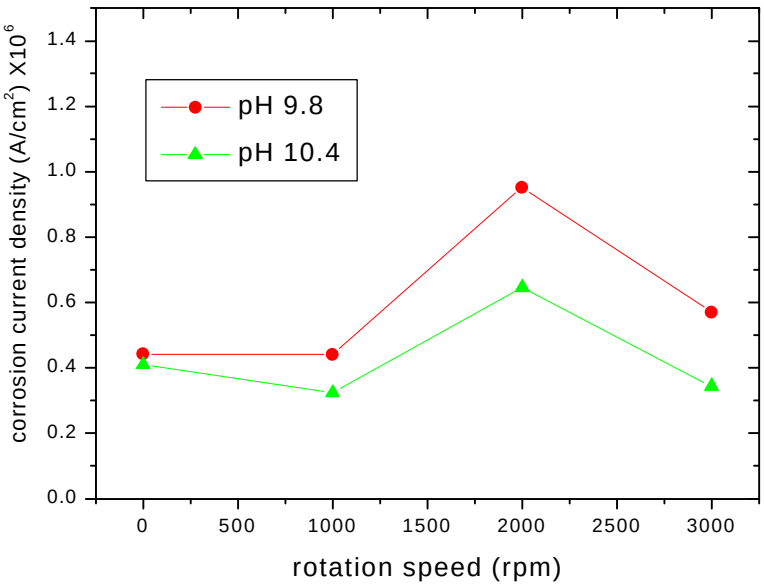

Figure 8. Results of linear polarization with different pH condition and rotating velocity

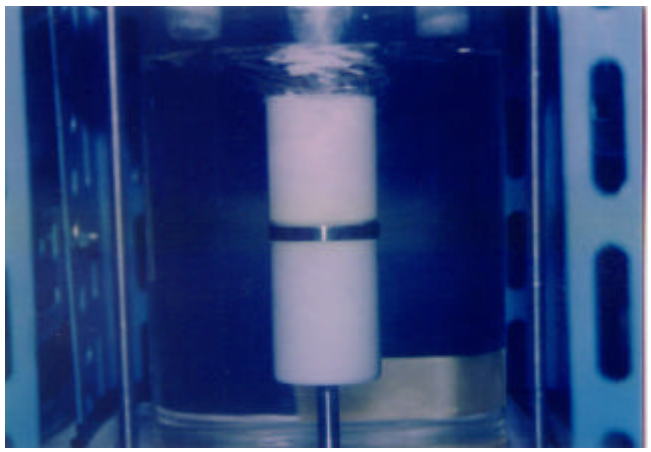

(a)

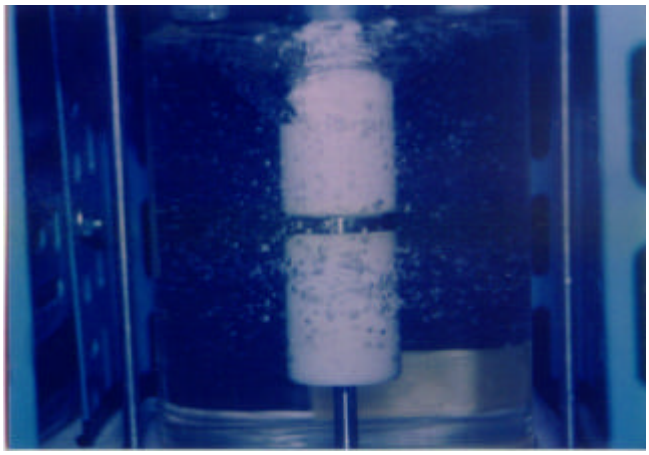

(b)

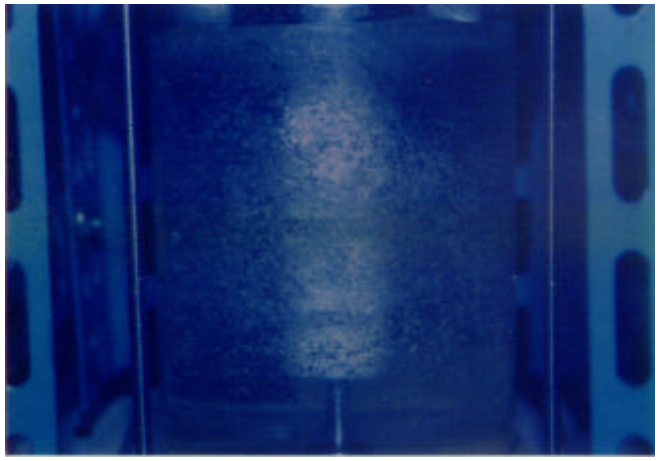

(c)

Figure 9. Flow Pattern of RCE (a) 1500rpm (b) 2500rpm (c) 3000rpm